

Power Spectrum Fitting For Image Restoration

José Luis Crespo

Abstract—In this work we use some well known statistic properties of natural images to present a simple but useful way of restoring degraded single images. It is based on the Fourier spectrum property of decaying exponentially for increasing frequencies.

The main idea is to leave the phase information untouched and to adapt the amplitudes so they fit a decaying law. This approach may seem too naive but it is capable of quite a decent restoration for images that usually are tackled by techniques such as blind deconvolution, often computationally expensive. It only delivers upon the user to choose a linear or parabolic fit in a log-log diagram.

Index Terms—Image restoration, Image enhancement

I. INTRODUCTION

IMAGE restoration is an important topic in research because of the need of improving the quality of blurred images. This problem has been reviewed in [1], [2].

Although many advances have been made, there are still occasions where degraded images do not get restored properly. Even when state of the art methods can actually give a decent result, some tweaking of parameters is required, and, since the top performing methods are usually computationally demanding, getting a final good restoration takes a lot of time.

In this work we show a computationally cheap way of achieving quite a good result, that works with many commonly found degraded images. Sometimes this result is not good enough and then the computationally demanding methods should be taken.

In section II we briefly review the topics that are involved. Then in section III we present our method. In section IV we show some results, and the possibilities for further research are discussed in section V.

II. PREVIOUS RESEARCH

A. Image restoration

Image degradation is a common problem that may be caused by noise, focusing defects or perturbations to the imaging device in the time it is taking the picture. We will briefly describe here the problem and the proposed solutions. See [3] for in-depth details, and [4] for an updated record.

The field of image restoration is dominated by the Fourier filtering approach, where a suitable filter is applied to the image in order to obtain the restored version. In this approach, image degradation in the Fourier domain is modeled as

$$g = Hf + a$$

where f corresponds to the original image, H to the perturbation, a corresponds to noise and g to the final distorted image.

J. L. Crespo is with the University of Cantabria, Avda. Los Castros, s/n, 39005 Santander, Spain, e-mail: crespoj@unican.es

If the exact nature of damage in the image is known, an inverse filtering approach might look sufficient, but, unfortunately, the ever present noise makes this very unstable, and the results are often quite bad. Then a regularized approach is needed. Some common ways for stable deconvolution are Wiener, Lucy-Richardson and blind deconvolution.

Wiener filtering [5] corresponds to a least squares approach that uses information about the PSF where noise amplification is prevented by adjusting the signal-to-noise ratio. See, for example, [6] for details.

Lucy-Richardson algorithm [7] iterates maximizing the likelihood that the resulting image, when convolved with the PSF (which is given) is an instance of the blurred image, assuming Poisson noise statistics. It is usually less affected by noise than the Wiener deconvolution. See [3] for details.

In both previous algorithms the degradation's PSF is known. When this is not the case, the user should start with an estimating effort. The other option is the blind deconvolution algorithm [8], where the PSF is found together with the restored image. Here the user is expected to have only an estimate of the PSF size. This is critical, and one of the recent proposals is [9] Improvements have been made for particular degradation models, such as [10].

There are also deblurring algorithms that are not Fourier based but wavelet-based [11]–[14]

A recent advanced deblurring algorithm can be reviewed in [15]

B. Natural image spectra statistics

We are going to focus on the 1D Fourier spectrum statistics. Other statistics of natural images can be reviewed in [16]

If we take the discrete Fourier transform of an image, we will have a function with amplitude and phase:

$$\mathcal{F}[I(f_x, f_y)] = A(f_x, f_y)e^{j\Phi(f_x, f_y)}$$

If we perform the rotational average of the amplitude within the two dimensional frequency plane we have a 1-D spectral power signal. This signal has been known for long to follow a power law in natural images. It was first observed by television engineers in the 50's [17], [18] and it has been revisited many times [19]–[23]. When considering image ensembles (let's remark that: ensembles) it often follows a decaying law that can be expressed as

$$\log(A) = -a \log(f) + b$$

or

$$A(f) = \frac{As}{f^a}$$

where a happens to be near 2 in many image ensembles (but not all, as it has also been studied). This a exponent is

sometimes used to describe the textures of images [24], [25]: higher values correspond to coarse textures and smaller values to finer grain ones. It also varies with different types of scenes [26]–[29]. Some empirically found averages are:

[26]	Man-made	vegetation	road	sky
	2.3	1.8	1.4	1

[29]	Forest	close-up meadow	distant meadow
	2.15	2.23	2.4

In [27] the a exponent is shown for different types of scenes, along with its orientation change.

It can be seen that different authors have found different slopes for similar categories, such as vegetation and forest.

Considering individual images, as it is our intent, we can see that in [30] departures of the straight line fit are reported. Some examples show how, for instance, images that are packed with small objects (no large objects at all, like a picture of a grass field) tend to be convex. In [31] it was already observed that individual images have different slopes and even curvature.

Considering the orientation influence, [23] showed that taking into account the orientation variation of the power spectra did not produce significant gains. [32] showed that, in different types of scenes, the type of anisotropy was different, but there is no clear law to fit. [28] show different shapes for different scenes, though the variation is quite large and it has not been pursued here.

In [22], [33] the reason behind that law was attributed to the nature of usual images, that are formed of objects with different sizes that overlap located at different distances. [30] studied a wide collection of images and concluded that it was only because of the usual type of imagery in which we are interested, and showed how different type of images have different decaying properties. The power law can be a manifestation of the fractal or scale invariant nature of images. There has been debate [34], [35] on the range of frequencies where this law was applicable, and whether the cause were edges or object distribution. Probably, it is not valid for very low frequencies.

Nevertheless, we won't be concerned with these limitations, since we will restrict ourselves to images acquired with commercial cameras, where the lowest frequencies are not that low, and we will let the user choose the starting frequency for the model to be valid.

This law has already been applied for categorization and classification [28]. It has also been used model the visual processing system [21], [36], [37] and to detect specific types of blurring in images [38], also in [39], where it is shown how blurred spots tend to have a lower a exponent, that is, sharper decrease.

There have been applications of these power law to restoration: [40] has some mechanics which are similar to the ones that we will produce, but they basically take the square root of the amplitude. [41] force the image to follow a power-law, but they impose a specific degradation model. As we will show below, even without a degradation model we can go a great deal to restoration. In [11] we can see an approach similar to ours, but they only use the linear log-log fit, they impose a

parametric PSF and finally they take these parameters to feed a deconvolution algorithm. In contrast, here we do not presume any specific PSF, we admit curvature in the log-log fit, and we directly force the image to follow a law. Note that [11]'s images are satellite images whereas we are dealing here with standard photographs.

III. MODEL FORMULATION AND IMPLEMENTATION

We notate the image by $I(x, y)$ and its Fourier transform by $F(w_x, w_y)$, that is,

$$F(w_x, w_y) = \mathcal{F}(I(x, y)) = A(w_x, w_y)e^{i\Phi(w_x, w_y)}$$

Then, let's set the phase information apart and let's take the amplitude $A(w_x, w_y)$. Now, if we shift the frequency coordinates to polar form we have $A(w_r, w_\theta)$. In order to get the average across the angular component we would do:

$$\overline{A(w_r)} = \frac{\oint A(w_r, w_\theta)d\theta}{\oint d\theta}$$

In the discrete case we sum through angles.

If we plot this function in a log-log diagram, we can see whether it fits the expected law.

Some random examples drawn from the 15 scene dataset [27], [42], [43] are shown in fig. 1, together with their 1D radial spectrum. These are not degraded, so they are examples of real radial spectra. We have used the [44] Matlab implementation to obtain these plots.

As it can be seen, individual slopes may vary, and the high frequency half of the log-log plot (roughly 90% of the equally sized frequency bins) are not always so linear. Sometimes a straight line seem to be a good fit, but sometimes a more concave shape is shown. Convex shapes are quite infrequent for the type of images commonly seen in everyday photographs.

We will start assuming we are working with common natural images. They may have the near -2 constant slope factor or maybe another factor or maybe a parabolic decay.

The so well known linear fit in the log-log diagram corresponds to the classic power-law:

$$\overline{A(w_r)} = \Gamma w_r^\alpha$$

If, instead, we use a parabolic fit, the it turns into:

$$\overline{A(w_r)} = \Gamma w_r^{\alpha + \beta \log w_r}$$

The algorithm for deblurring the image is presented in fig 2

What we propose is to take the radial histogram of a degraded picture and change it so it matches one of the two previous fits. This is not an automatic method where the computer takes all decisions. It is an interactive method, but this is not a serious drawback because of two reasons:

- It is easy to provide a reasonable choice
- The result is quickly computed, so a new histogram shape can be tried if necessary

We will interactively define a desired shape for the radial histogram (steps 7 to 10). This will lead to a given gain for

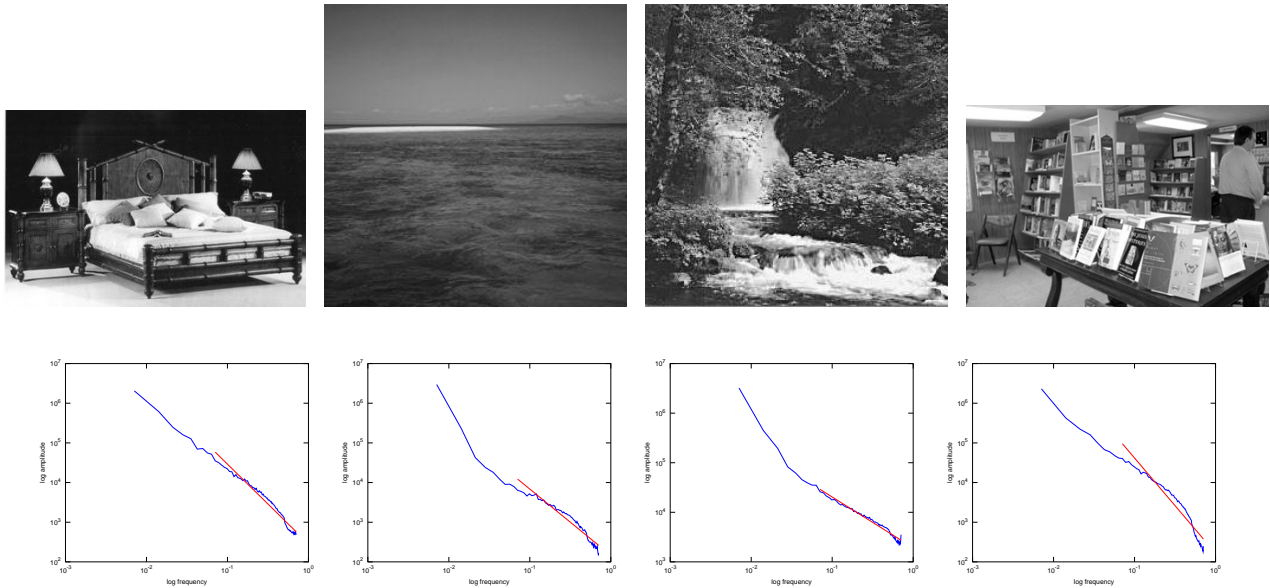


Fig. 1. Examples of photographs and their 1D spectrum

Require: user to choose degree of fit (1 for linear, 2 for parabolic)

- 1: **if** it is a color image **then**
- 2: Take the Value channel out of the HSV representation
- 3: **end if**
- 4: Produce the Discrete Fourier Transform of the image
- 5: Average rotationally the amplitude of the DFT for every radial bin, using 100 bins
- 6: **repeat**
- 7: plot the log-log plot of averaged amplitude versus frequency
- 8: let the user choose a number of points for the fit (at least two more than the degree of the fit). They are not necessarily part of the amplitude line.
- 9: fit a straight line or a parabola to the points the user provided (restricted between the interval of frequencies spanned by the user-provided points)
- 10: plot the resulting fit, on top of the original amplitude versus frequency plot
- 11: **until** user is satisfied with the plot
- 12: Define gain as the ratio between the fit and the original amplitude
- 13: **if** original image was in color **then**
- 14: Apply gain to the amplitudes of DFT of each of the RGB channels (within the frequency span defined by the user)
- 15: Deblur each channel by taking the inverse DFT of the new amplitude and the original phase
- 16: **else**
- 17: Apply gain to the original amplitude (within the frequency span defined by the user)
- 18: Deblur the image by taking the inverse DFT of the new amplitude and the original phase
- 19: **end if**
- 20: Make sure the result is valid by discarding any imaginary component and clipping the results to the allowed image range

Fig. 2. Proposed deblurring algorithm

each frequency band (step 12), defining an "enhancing" or "restoration" filter that we will apply to the image (steps 13 to 20). The way it is built implies that:

- The restoration filter does not affect phase. The original phase information is left as is.
- Since we take the filter from a 1D spectrum, it will be radially symmetric
- We get directly a restoration filter, not a PSF of the degradation

These may be considered serious limitations, but our results

show that the approach is quite robust and effective, though it is not perfect, and cannot cope with a serious departure of the first two assumptions. That is we need that phase information is mostly valid, and the perturbation is not too far from radial symmetry. Most failures of our method correspond to synthetic examples, where theoretical PSF's are used. Apparently, real life PSF's are not so far from the symmetric case.

Summarizing our method: we produce a desired histogram by taking a first or second order fit to the points that the user enters in the log-log plot and, once the user accepts the shape,

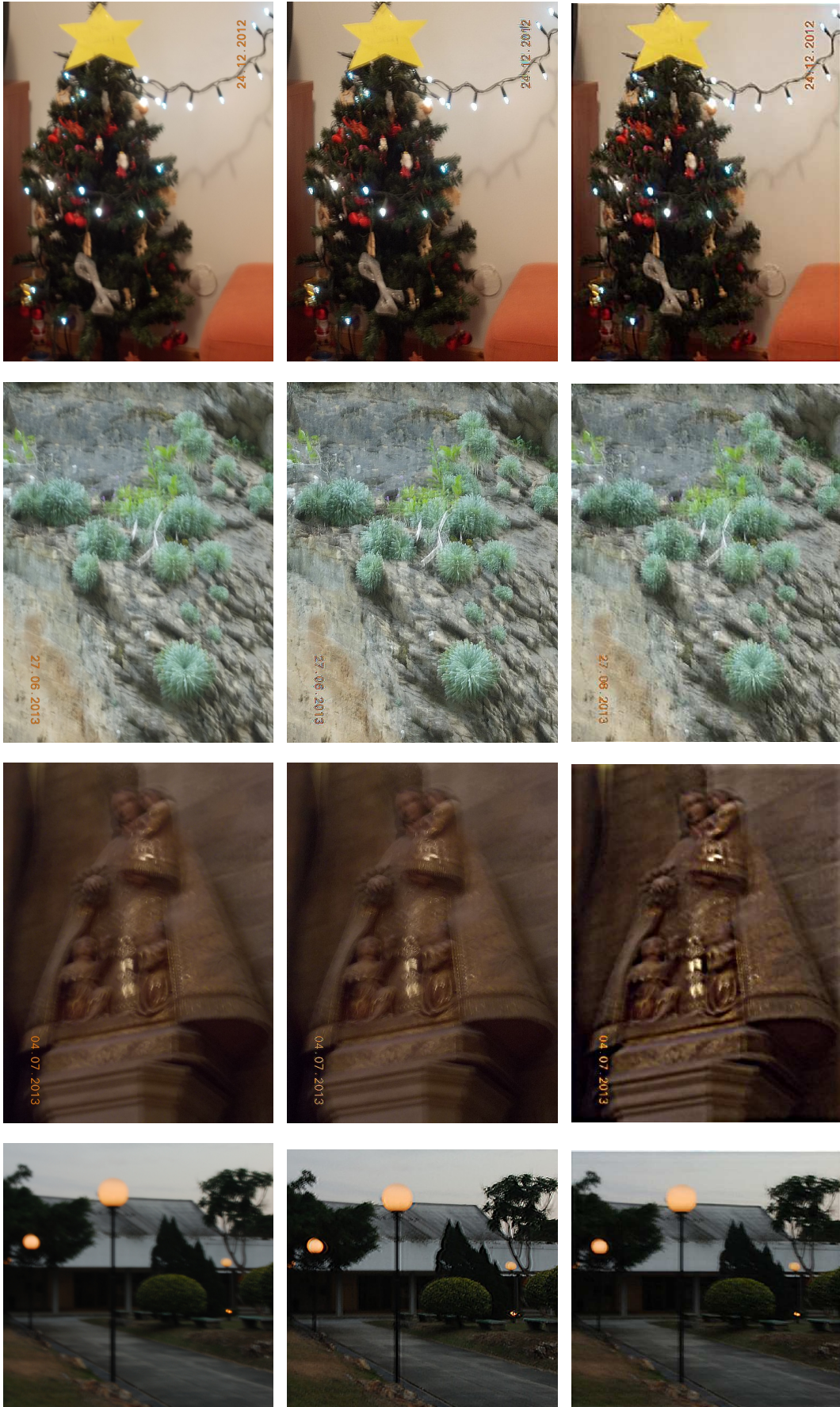


Fig. 3. Results with some sample images. Left column are original images, center column images restored with [15] method and right column are restored with proposed method. Last row is an example taken from [15] and the rest are degraded images taken from a personal collection, taken with a simple digital camera.

we find the needed gain in each affected frequency band. For color images we calculate this in the value channel of the HSV representation of the image, and the same gain is then applied to all three RGB channels. All gain operations are done in the frequency domain, and the inverse Fourier transform is taken to recover the original image, which is clipped if some value fails to be inside the allowed range.

IV. RESULTS

We have implemented the method as a Matlab function and have measured the time it takes to deblur images. In figure 3 we can see the results of applying the above mentioned procedure to some sample pictures. For comparison purposes, we present also the results of applying a state of the art blind deconvolution restoring algorithm [15]. Note that this is a compiled executable program, not a Matlab function.

Though blind deconvolution is intended to be a fully automatic, no user-tweaking algorithm, some tweaking is permitted and sometimes necessary or at least recommended. Each method has some parameters you can play with. In the particular method of [15] you need an estimation of the PSF size (common to all blind deconvolution techniques) and the noise level (in some other techniques that follow a bayesian framework you may need to give some information characterizing the image prior). In these experiments, for the initial PSF size we have used a simple visual estimation, and we have left the noise level at its default value. Since this method needs large memory for the images, we have reduced sizes if needed, to about 300 Kpx

Considering the computation time, the non interactive part of our method is solved in Matlab, in the computer we used, most times between 1 and 2 seconds. The [15] method uses a compiled program that solved the problem in around 2 minutes in the same computer, with some difficult cases (large PSF size) requiring even 30 minutes.

Since these are actual degraded pictures, in most cases there is no ground truth available. This also means that the actual perturbation may be of any kind, including the nonlinear case. Other than the visual appearance, we made an attempt of objective image quality assessment, by using the IQM measure [45] of the images. On the average the [15] method gave an improvement with a factor of more than 2 in the first attempt. The proposed method gave an improvement with a factor of more than 3 with most of the images in a single attempt and with one out of each four, in two attempts.

As it can be seen, this method produces results that are comparable to more sophisticated methods, with much less computational effort.

Next, we show some sensitivity results. studying how the outcome can vary with the following choices:

- lowest and highest frequency to filter
- vertical displacement in the log-log plot
- higher or lower exponents of the power-law to fit

We use the 2260 (third row in Fig. 3) image as an example for these tests. In figure Fig. 4 we see the fit and the corresponding result

As can be seen, all choices improve the original image. No big differences are produced. The choice of highest frequency

to filter doesn't make much of a difference, provided you don't get way too short. The most influential factor seems to be the lowest frequency to filter. For the particular image shown in the figure, a parabolic fit makes a better improvement. Hence, a recommended approach for the user would be to try first a linear and a parabolic fit in a sensible frequency interval, this means roughly the rightmost half in the log-log plot. Then, choose the best one and try varying the lowest frequency. Good hints for this are the bending points that may show up in the original amplitude plot; great accuracy is not required. All this process can easily be performed in a minute.

V. CONCLUSIONS

A simple but effective restoration method has been proposed. It is well suited to common real images with common real degradations. It works pretty well with very little previous knowledge.

An interesting further research will be the fitting of an image to the closest point in the natural image manifold.

It remains an open question whether there is a way to improve quality by taking into account different directions. If we don't sum radially for all frequencies, but retain the direction, we may be able to apply selective filtering for different directions. In a preliminary attempt we have found no advantages, because data are more sensitive to noise, since there is no a summing operation, which has the side effect of canceling some noise. It would be interesting to follow [28], to fit orientations and overall size, according to the methods described in [23].

REFERENCES

- [1] P. A. Patil and R.B.Wagh, "Review of blind image restoration methods," *World Journal of Science and Technology*, vol. 2, no. 3, pp. 168–170, 2012.
- [2] X. L. Bahadir Kursat Gunturk, Ed., *Image Restoration Fundamentals and Advances*. CRC Press, 2012.
- [3] A. Katsaggelos, *Digital Image Restoration*. Springer Verlag, 1991.
- [4] A. Histace, *Image Restoration - Recent Advances and Applications*, Apr. 04 2012. [Online]. Available: <http://hal.archives-ouvertes.fr/hal-00685358>
- [5] A. Rosenfeld and A. Kak, *Digital Picture Processing*, 2nd ed. Academic Press, 1982.
- [6] González and Woods, *Digital Image Processing*, 3rd ed. Prentice Hall, 2008.
- [7] L. B. Lucy, "An iterative technique for the rectification of observed distributions," *Astronomical Journal*, vol. 79, no. 6, pp. 745–754, 1974.
- [8] D. Kundur and D. Hatzinakos, "Blind image deconvolution," *IEEE Signal Processing Magazine*, 1996.
- [9] U. M. M. Fahmy, G. Raheem and O. Fahmy, "A new fast iterative blind deconvolution algorithm," *Journal of Signal and Information Processing*, vol. 3, no. 1, pp. 98–108, 2012, doi: 10.4236/jsip.2012.31013.
- [10] R. F. et al, "Removing camera shake from a single image." SIGGRAPH 2006, 2006.
- [11] X. bing Chen, S. zhi Yang, X. hua Wang, and Y. li Qiao, "Satellite image blind restoration based on surface fitting and iterative multishrinkage method in redundant wavelet domain," *Optik - International Journal for Light and Electron Optics*, vol. 121, no. 21, pp. 1909 – 1911, 2010. [Online]. Available: <http://www.sciencedirect.com/science/article/pii/S003040260900240X>
- [12] M. Fornasier, Y. Kim, A. Langer, and C.-B. Schönlieb, "Wavelet decomposition method for 1/2tv-image deblurring," *SIAM Journal on Imaging Sciences*, vol. 5, no. 3, pp. 857–885, 2012, cited By (since 1996)0.
- [13] Z. Wang, "Image deblurring regularized by wavelet probability shrink," 2011, pp. 610–613, cited By (since 1996)0.

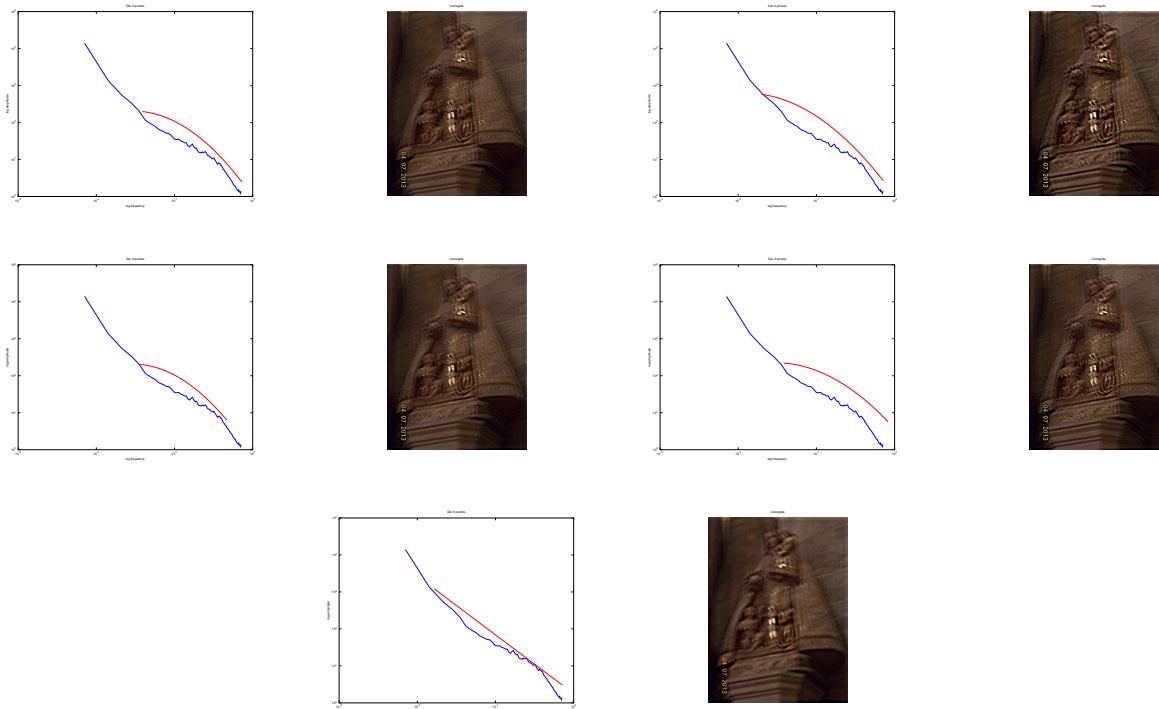


Fig. 4. Sensitivity analysis to some of the fitting possibilities. Spectra choice shown on the left and resulting image shown on the right

- [14] H. Yin and H. Liu, "A bregman iterative regularization method for wavelet-based image deblurring," *International Journal of Wavelets, Multiresolution and Information Processing*, vol. 8, no. 3, pp. 485–499, 2010, cited By (since 1996)3.
- [15] A. A. Qi Shan, Jiaya Jia, "High-quality motion deblurring from a single image," *ACM Transactions on Graphics*, vol. 27, no. 3, August 2008, article 73.
- [16] J. Gluckman, "Kurtosis and the phase structure of images," in *3rd International Workshop on Statistical and Computational Theories of Vision*, 2003, p. 2003.
- [17] N. Deriugin, "The power spectrum and the correlation function of the television signal," *Telecommunications*, vol. 1, pp. 1–12, 1956.
- [18] E. Kretzmer, "Statistics of television signals," *Bell Syst. Tech.*, vol. 31, pp. 751–763, 1952.
- [19] D. J. Field, "Relations between the statistics of natural images and the response properties of cortical cells," *J. Opt. Soc. Am. A*, vol. 4, pp. 2379–2394, 1987.
- [20] G. J. Burton and I. R. Moorhead, "Color and spatial structure in natural scenes," *Applied Optics*, vol. 26, pp. 157–170, 1987.
- [21] J. H. v. Hateren, "Theoretical predictions of spatiotemporal receptive fields of fly lms, and experimental validation," *Comparative Physiology A*, vol. 171, pp. 157–170, 1992.
- [22] D. L. Ruderman, "Origins of scaling in natural images," *Vision Res.*, vol. 37, no. 23, pp. 3385–3398, 1997.
- [23] A. van der Schaaf and J. van Hateren, "Modeling of the power spectra of natural images: Statistics and information," *Vision Research*, no. 36, pp. 2759–2770, 1996.
- [24] T. B. H. Billock V.A., Cunningham D. W., "What visual discrimination of fractal textures can tell us about discrimination of camouflaged targets," in *Proceedings of Human Factors Issues: In Combat Identification and in Image Analysis Using Unmanned Aerial Vehicles*, 2008.
- [25] H. P. R. Billock V. A., Cunningham D. W., "Perception of spatiotemporal random fractals: an extension of colorimetric methods to the study of dynamic texture," *Journal of the Optical Society of America A*, vol. 18, no. 10, pp. 2404–2413, 2001.
- [26] M. D. Huang J., "Image statistics for the british aerospace segmented database," Division of Applied Math, Brown University, Tech. Rep., 1999.
- [27] A. T. A. Oliva, "Modeling the shape of the scene: A holistic representation of the spatial envelope," *International Journal of Computer Vision*, vol. 42, no. 3, pp. 145–175, 2001.
- [28] G.-D. A. Oliva A., Torralba A. and H. J., "Global semantic classification using power spectrum templates," in *Proceedings of The Challenge of Image Retrieval*, ser. Electronic Workshops in Computing. Newcastle: Springer-Verlag, 1999.
- [29] M. E. Webster M., "Contrast adaptation and the spatial structure of natural images," *Journal of the Optical Society of America A*, vol. 14, pp. 2355–2366, 1997.
- [30] M. S. Langer, "Large-scale failures of $f^{-\alpha}$ scaling in natural image spectra," *J. Opt. Soc. Am. A*, vol. 17, no. 1, pp. 28–33, January 2000.
- [31] T. Y. . C. T. Tolhurst D. J., "Amplitude spectra of natural images," *Ophthalmic and Physiological Optics*, vol. 12, pp. 229–232, 1992.
- [32] M. M. Switkes E. and S. J.A., "Spatial frequency analysis of the visual environment: anisotropy and the car-centered environment hypothesis," *Vision Research*, no. 18, pp. 1393–1399, 1978.
- [33] A. Lee and D. Mumford, "Occlusion models for natural images: A statistical study of scale invariant dead leaves model," *International Journal of Computer Vision*, vol. 41, no. 1,2, 2001.
- [34] C. W. T. Norberto M Grzywacz, Rosario M Balboa, "Author's reply to ruderman's comments," *Vision Research*, vol. 42, no. 25, pp. 2803–2805, Nov. 2002.
- [35] D. L. Ruderman, "Comments to grzywacz et al. article," *Vision Research*, vol. 42, no. 25, pp. 2799–2801, Nov. 2002.
- [36] J. H. v. Hateren, "Spatiotemporal contrast sensitivity of early vision," *Vision Research*, vol. 33, pp. 257–267, 1993.
- [37] J. J. Atick and A. N. Redlich, "Towards a theory of early visual processing," *Neural Computation*, vol. 2, pp. 308–320, 1992.
- [38] A. S. Carasso, "Direct blind deconvolution," *SIAM J. Appl. Math.*, vol. 61, no. 6, pp. 1980–2007, 2001.
- [39] R. Liu, Z. Li, and J. Jia, "Image partial blur detection and classification," in *Computer Vision and Pattern Recognition, 2008. CVPR 2008. IEEE Conference on*. IEEE, 2008, pp. 1–8.
- [40] N. M. N. James N. Caron and C. J. Rollins, "Noniterative blind data restoration by use of an extracted filter function," *Applied Optics*, vol. 41, no. 32, pp. 6884–6889, November 2002.
- [41] A. Jalobeanu, L. Blanc-féraud, J. Zerubia, and S. Antipolis, "Estimation of blur and noise parameters in remote sensing," in *Proc. of Int. Conf. on Acoustics, Speech and Signal Processing*, 2002, pp. 249–256.
- [42] L. Fei-Fei and P. Perona, "A bayesian hierarchical model for learning natural scene categories," in *CVPR*, 2005.
- [43] C. S. S. Lazebnik and J. Ponce, "Beyond bags of features: Spatial

pyramid matching for recognizing natural scene categories,” in *CVPR*, 2006.

- [44] P. D. Kovesi, “MATLAB and Octave functions for computer vision and image processing,” Centre for Exploration Targeting, School of Earth and Environment, The University of Western Australia, available from: <<http://www.csse.uwa.edu.au/~pk/research/matlabfns/>>.
- [45] N. Nill and B. Bouzas, “Objective image quality measure derived from digital image power spectra,” *Optical Engineering*, vol. 31, pp. 813–825, April 1992.



José L. Crespo Received its B.S. and Ph.D. in Engineering at the University of Cantabria.

He worked as a consultant in Civil Engineering projects. He is currently a professor at the University of Cantabria (Santander, Spain) where he works in neural networks and image processing.